U.S. Air Force Research

U.S. Department of Defense

2012

Char-forming behavior of nanofibrillated cellulose treated with *glycidyl phenyl* POSS

Douglas M. Fox
American University, National Institute of Standards and Technology

Jieun Lee
American University

Mauro Zammarano
American University, National Institute of Standards and Technology, National Institute of Standards and Technology

Dimitris Katsoulis
Midland

Donald V. Eldred
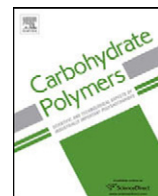*Midland*

See next page for additional authors

Follow this and additional works at: http://digitalcommons.unl.edu/usafresearch

Authors

Douglas M. Fox, Jieun Lee, Mauro Zammarano, Dimitris Katsoulis, Donald V. Eldred, Luke M. Haverhals, Paul C. Trulove, Hugh C. DeLong, and Jeffery W. Gilman

Char-forming behavior of nanofibrillated cellulose treated with glycidyl phenyl POSS

Douglas M. Fox [a,b,*], Jieun Lee [a], Mauro Zammarano [a,b,c], Dimitris Katsoulis [d], Donald V. Eldred [d], Luke M. Haverhals [e], Paul C. Trulove [e], Hugh C. De Long [f], Jeffrey W. Gilman [c]

[a] Department of Chemistry, American University, Washington, DC 20016, USA
[b] Fire Research Division, Engineering Laboratory, National Institute of Standards and Technology, Gaithersburg, MD 20899, USA
[c] Polymers Division, Material Measurement Laboratory, National Institute of Standards and Technology, Gaithersburg, MD 20899, USA
[d] Dow Corning Corporation, Midland, MI 48686, USA
[e] Chemistry Department, U.S. Naval Academy, Annapolis, MD 21402, USA
[f] Air Force Office of Scientific Research, Arlington, VA 22203, USA

ARTICLE INFO

ABSTRACT

Cellulose-reinforced composites have received much attention due to their structural reinforcing, light weight, biodegradable, non-toxic, low cost and recyclable characteristics. However, the tendency for cellulose to aggregate and its poor dispersion in many polymers, such as polystyrene, continues to be one of the most challenging roadblocks to large scale production and use of cellulose-polymer composites. In this study, nanofibrillated cellulose (NFC) is modified using GlycidylPhenyl-POSS (a polyhedral oligomeric silsesquioxane). The product yield, morphology, and crystallinity are characterized using a variety of spectroscopy and microscopy techniques. Thermal analyses are performed using thermal gravimetric analysis and pyrolysis combustion flow calorimetry.

1. Introduction

Cellulose, hemicelluloses, and lignins are collectively known as lignocellulosic materials. Plants are predominantly composed of lignocellulosic materials, making cellulose the most abundant natural compound on earth. Cellulose is the primary component providing strength to wood and other plant structures. As a result, there are countless studies on preparing cellulose-polymer composites for improving the mechanical properties of polymers. Despite this potential, there are still some limitations to its use in commodity plastics: the addition of cellulose fibers often results in a decrease in fracture toughness (Clemons, Caulfield, & Giacomin, 1999), its hydrophilicity can lead to high moisture absorption and poor interfacial adhesion (Girones et al., 2007; Joseph, Thomas, & Pavithran, 1996; Samir, Alloin, & Dufresne, 2005), its low thermal stability limits processing and operating temperatures to below 200 °C (Samir et al., 2005; Wu, Yu, Chan, Kim, & Mai, 2000) and its high polarity leads to incompatibilities with the most common polymers, such as polyethylene, polypropylene, and polystyrene.

For decades, there has been interest in extracting energy from biomass sources. One of the simplest and most inexpensive methods available today is the pyrolysis of biomass to form high energy density fuels as chars and carbon tars or oils. In an effort to increase the usable high energy density fuels from biomass, the pyrolysis of lignocellulosic materials has been studied in detail in recent years (Antal & Varhegyi, 1995; Blasi, 2008; Saddawi, Jones, Williams, & Wojtowicz, 2010). Analyses have indicated a negative correlation between thermal stability temperatures and char yields. Under anaerobic conditions, lignin decomposes first (T_d = 200 °C, char = 45% by mass), followed by hemicelluloses (T_d = 250 °C, char 20% by mass), and finally cellulose (T_d = 320 °C, char 6% by mass) (Ramiah, 1970; Yang, Yan, Chen, Lee, & Zheng, 2007). Cellulose is the main component of biomass, but yields the lowest amount of solid or liquid residues. A variety of processing conditions and modifications have been used to increase char formation during cellulose pyrolysis (Khelfa, Finqueneisel, Auber, & Weber, 2008; Shimada, Kawamoto, & Saka, 2008; Tang & Eickner, 1968; Wanna & Powell, 1993). Many of these do not significantly increase the char yield, and the most effective (such as addition of alkali and alkaline metal salts) come at the expense of reduced thermal stability. For the generation of solid and liquid fuels, this may be beneficial, but it also severely limits the usefulness of cellulose as a flame retardant (FR) for polymers.

* Corresponding author at: Department of Chemistry, American University, Washington, DC 20016, USA. Tel.: +1 202 885 1735; fax: +1 202 885 1752.
E-mail address: dfox@american.edu (D.M. Fox).

Polyhedral oligomeric silsesquioxanes (POSS) are a class of compounds with an inorganic silicon – oxygen core and bulky organic substituents on the outer surface. They have gained attention as a polymeric additive principally because they can be modified to achieve good interfacial adhesion with the polymer matrix (Phillips, Haddad, & Tomczak, 2004; Zhao, Fu, & Liu, 2008) and, once well dispersed, have the ability to improve a variety of polymer properties, including increased oxidative resistance, increased toughness, increased thermal stability, and reduced flammability (Li et al., 2001; Schwab & Lichtenhan, 1998; Zheng, Farris, & Coughlin, 2001). The exterior organic layer allows POSS to be incorporated in hydrophobic polymers, such as polypropylene (Fina, Tabuani, Frache, & Camino, 2005; Zheng et al., 2001; Zhou, Cui, Zhang, Zhang, & Yin, 2008) and polystyrene (Cardoen & Coughlin, 2004; Liu et al., 2007; Wu, Haddad, Kim, & Mather, 2007). Due to the availability of POSS molecules with a variety of both reactive and non-reactive substituent functionalities, polymer composites have been synthesized using copolymerization, grafting, or simply blending techniques (Li et al., 2001).

In cone calorimetry experiments, POSS has been shown to reduce polymer flammability both as a single nanofiller and as a synergist in phosphorus containing flame retarded polymers. Researchers found that the addition of 30% by mass of octa(tetramethylammonium) POSS to polystyrene significantly improved the fire retardancy of the polymer by reducing the peak heat release rate by more than half, increasing the peak decomposition temperature by 10 °C, and increasing char yield by 25% (Liu et al., 2007). Flame retardant effects were noticeable with as little as 5% POSS by mass. In epoxy matrixes, additions of less than 10% POSS by mass reduced the peak heat release rate by close to 50% (Franchini, Galy, Gerard, Tabuani, & Medici, 2009). POSS has also been shown to be effective as a flame retardant synergist in polymers. Gerard, Fontaine, and Bourbigot (2011) has very recently observed a very large synergistic effect in flame retardancy when POSS is added to intumescent epoxy. Vannier and coworkers found that the addition of 2% by mass of Octamethyl POSS to poly(ethylene terephthalate) flame retarded with a commercial based zinc phosphinate compound further reduced peak heat release rate by half and increased the limiting oxygen index by nearly 20% (Vannier et al., 2008). And, Chigwada, Jash, Jiang, & Wilkie (2005) found that additions of 5% Vinyl POSS by mass to tricresylphosphate–poly(vinyl ester) composites resulted in significant increases in char and modest reductions in peak heat release rate. In these studies, the mechanisms have been identified as the formation of a silica rich, ceramic-like char layer at the surface of the burning front of the material (Bourbigot, Duquesne, & Jama, 2006; Fina, Abbenhuis, Tabuani, & Camino, 2006; Qian et al., in press). This improvement in flammability properties does not come at an expense of processability (Li et al., 2001).

Most POSS monomers have one organic substituent linked to a reactive end-group, which can be used to graft the POSS molecules to polymers and other molecules. Three classes of POSS molecules that can potentially react with the cellulosic hydroxyl groups are isocyanates, epoxides and amic acids. By covalently bonding POSS molecules onto the cellulose chains, the benefits of both nanoparticles may be realized. The addition of cellulose should lead to an increase in char yield while the addition of POSS should lead to improved dispersion of the nanoparticles and formation of a ceramic char layer (Bourgibot et al., 2006; Fox et al., 2007), which may further lower the flammability of the nanocomposite. The hybrid nanoparticle may improve processing properties over the addition of cellulose or POSS alone. The addition of cellulose leads to improved tensile and Young's modulus properties, but suffers from decreased fracture toughness and can lead to reduced crystallinity (Ljungberg et al., 2005; Jonoobi, Harun, Matthew, & Oksman, 2010). POSS has been found to increase modulus, tensile

strength, and fracture toughness, but tend to decrease chain mobility and increase crystallinity (Wu, Haddad, & Mather, 2009; Zhang et al., 2002). The rigidity of POSS molecules imbues surface toughness (Zhang et al., 2002), which may reduce interfacial stress. The incorporation of POSS can also reduce stiffness and strength when the POSS begins to agglomerate due to higher concentrations or poor compatibility with the polymer matrix. The key to improved mechanical and rheological properties appears to lie on the ability to match the organic substituents on POSS with the matrix polymers and keeping the additions of POSS to a minimum, resulting in good interfacial adhesion (Phillips et al., 2004; Zhao et al., 2008).

It is desirable that this work will further the development of sustainable flame retardants with low toxicity for use in polymer nanocomposites. POSS molecules have been found to exhibit low toxicity levels in drug carrier (McCusker, Carroll, & Rotello, 2005) and decomposition studies (Fina et al., 2006; Liu, Hu, Song, Gu, & Ni, 2010). Previous work on layered silicates (clay) exchanged with POSS modified imidazolium cations has shown significant improvements in thermal stability over conventionally exchanged clays (Fox et al., 2007). However, strong POSS aggregation prevented full exfoliation of the clay in polymers, reducing its fire retardant potential (Fox et al., 2011). Like layered silicates, cellulose can enhance mechanical properties, such as flexural strength and stiffness (Jonoobi et al., 2010; Tajvidi, Feizmand, Falk, & Felton, 2009). This is advantageous over other flame retardants (FRs), such as magnesium hydroxide and ammonium polyphosphate/pentaerythritol, which are known to reduce flexural and impact strength, elongation to break, and melt viscosity (Anna, Marosi Gy Bertalan Gy Marton, & Szep, 2002; Jiao et al., 2009; Li & He, 2004). For cellulose to be beneficial as a FR, charring must be enhanced with a minimal loss in the thermal stability temperature. Most modifications that enhance charring in cellulose, such as sulfonation (Roman & Winter, 2004), the addition of phosphorus containing compounds (Weil & Levchik, 2008), and non-durable metal halide addition (Khelfa et al., 2008; Shimada et al., 2008), have been shown to substantially reduce the thermal stability of the cellulose. As shown in this study, incorporation of POSS can enhance charring with limited loss in thermal stability.

The synthesis of POSS-modified cellulose using toluene (Fox et al., 2010a,b) and the preparation of cellulose encapsulated POSS using an ionic liquid (Fox et al., 2010a,b) has recently been reported. In the current study, the effects of the solvent choice, modifying agent, and modifier content on the ability to form nanofibrillated cellulose with enhanced charring abilities was investigated. Extent and quality of the substitution was examined using Fourier Transform Infrared Spectroscopy (FTIR), elemental analysis, X-ray diffraction (XRD), and solid state nuclear magnetic spectroscopy (SS-NMR). Fiber morphology and POSS distribution was monitored using scanning electron microscopy with electron dispersion spectroscopy (SEM-EDS). The ability of POSS to enhance char during pyrolysis of cellulose was examined by thermal gravimetric analysis (TGA), pyrolysis combustion flow calorimetry (PCFC), SEM-EDS, and X-ray spectroscopy (XPS). Use of the modified cellulose as a flame retardant additive in polymers such as poly(lactic acid) is currently under investigation.

2. Experimental

2.1. Materials

N,N-dimethylformamide/DMF (Aldrich, 99.8%), toluene (Acros, 99%), ethyl alcohol (Aaper, USP 200), (1,2-epoxy-3-phenoxypropane/glycicyl phenyl ether (Aldrich, 99%), diethoxy(3-glycidyloxypropyl)methylsilane/(EtO)$_2$(GlyOPr)MeSi (Aldrich, 97%), NaOH (Fisher, ACS grade), acetic acid (Aldrich, 99.8%), GlycidylPhenylPOSS/GlyPh$_7$POSS (Hybrid Plastics), and

OctaPhenyl POSS/Ph$_8$POSS (Hydbrid Plastics) were all used as received. De-ionized water (>16 MΩ) was obtained from a Barnsted E-pure 3-module water purification system. Nanofibrillated cellulose/L040-6 (prepared by fibrillating the ends of 6 mm length of Lyocell regenerated fibers until reaching an MSR drainage of 40 ml) was obtained from Engineered Fibers Technology. The nanofibrils had an average diameter between 50 nm and 100 nm. The received fibers contained some impurities, which were removed with consecutive washes in 1 M acetic acid, deionized water, and 50/50 (v:v) ethanol/water solutions. The fibers were then dried at 90 °C for 24 h and partially de-bundled manually prior to use.[1]

2.2. Modification of cellulose

Nanofibrillated cellulose fibers were modified with a glycidyl POSS compound using a procedure similar to that reported for phenyl glycidyl ether cellulose (McKelvey, Webre, & Klein, 1959). Cellulose (1 g) was alkaliated using a 15% by mass aqueous NaOH solution (20 mL) for 1 h. The Na-cellulose was filtered using a sintered glass crucible (4–8 μm), then was thoroughly washed with dry ethanol and filtered until its wet uptake was 200% by mass. The Na-cellulose was placed in a solvent (20 mL water, toluene, and DMF) and a modifying agent (between 0.33 g and 5 g) was added. The reaction mixture was heated to 90 °C for 24 h. The reaction mixture was filtered (filtrate saved for analysis) and soxhlet extracted with fresh solvent for 48 h. Excess solvent was squeezed out of the fibers, then the fibers were washed in a 60:40 (v:v) ethanol – deionized water mixture. The product was then neutralized with 0.5 mol/L acetic acid (40 mL) and soxhlet extracted 24 h with 60:40 (v:v) ethanol – deionized water to remove trace ions. The final product was dried in a conventional oven at 80 °C for 24 h.

2.3. Instrumentation

Infrared absorption spectra (FTIR) were collected using a Shimadzu FTIR-3800 Fourier transform infrared spectrometer equipped with a diffuse reflectance (DRIFT) sample holder. Samples (4% by mass) were hand ground in a pestle and mortar to a fine powder in KBr. The spectra were collected using an average of 64 scans with a spectral resolution of 2 cm^{-1}. All reported wavenumbers have an uncertainty of $2\sigma = \pm5$ cm^{-1}.

Elemental analysis was performed by Galbraith Laboratories, Inc. Carbon and hydrogen analyses were performed by the combustion method (GLI procedure ME-11) and silicon analysis was performed by ICP/AA (GLI procedure ME-70). All analyses were performed in duplicate on 50 ± 5 mg samples and the mean is reported here.

Nuclear magnetic spectra were acquired on a Varian Inova NMR spectrometer with ^{29}Si at 79.40 MHz and ^{13}C at 100.51 Mhz. Magic-angle spinning (MAS) and cross-polarization magic-angle spinning (CPMAS) measurements were made using the standard xpolvt1rho1 pulse sequence under a contact array ranging from 300 μs to 14,000 μs. Two Pulse Phase Modulated decoupling was applied to reduce dipolar interferences. Pulse repetition delay times of 5 s was used for CPMAS acquisitions while 45 s and 90 s was used for ^{13}C and ^{29}Si MAS data acquisitions respectively. Samples

were packed into 7 mm OD ZrO rotors and spun between 4250 and 5000 Hz. Accuracy and precision has not been determined.

Scanning Electron Microscopy (SEM) images were collected using a Joel JSM-6360LV low/high vacuum energy dispersive spectroscopy (EDS) microanalysis system. Samples were mounted on conductive tape without addition or sputter-coating the samples. Images were taken over three locations on the sample to ensure uniform representation of the topography.

Powder X-ray diffraction experiments were performed on a Bruker AXS D8 Powder diffractometer. The d-spacing was calculated from peak positions using Cu Kα radiation (λ = 0.15418 nm) and Bragg's Law. Samples were prepared by pressing (6 atm) 0.5 g in a hydraulic press at room temperature and mounting on a small clay sample. Standard X-ray measurements were performed over a 2θ range of 5–40° using a step size of 0.05° for 20 sec with an uncertainty of $2\sigma = \pm0.001°$.

Thermal stabilities were measured using a TA Instruments Q-500 Thermogravimetric Analyzer. 5.0 ± 0.2 mg samples were placed in open platinum pans and heated at a scan rate of 10 °C/min while purged with 100 mL/min N$_2$. The mean of three replicate measurements are reported. The temperature of both the onset (5% mass fraction loss) and peak mass loss rate have an uncertainty of $2\sigma = \pm3$ °C. All samples were held at 90 °C for 30 min prior to each scan to remove any residual water and, in the case of the thermal stability in nitrogen, to remove any residual oxygen from the furnace.

Pyrolysis-combustion flow calorimetry (PCFC) and X-ray spectroscopy (XPS) were performed by University of Dayton Research Institute. The PCFC samples (5 ± 0.1 mg) were tested with a Govmark MCC-2 microcombustion calorimeter at 1 °C/s heating rate under nitrogen from 200 °C to 600 °C using method A of ASTM D7309 (pyrolysis under nitrogen). Each sample was run in triplicate to evaluate reproducibility of the flammability measurements. The heat release capacity (HRC), total heat release (THR), peak heat release temperature (HRR), and char yield were determined with uncertainties of $\sigma = \pm6$ W/g, ±0.4 kJ/g, ±2 °C, and 1.7%. XPS of the cellulose samples was conducted with a Surface Science Labs SSX-100 XPS. This instrument has a focused, monochromatic aluminum X-ray source. A nominal X-ray spot size of 600 μm was used for this work. The powder samples were prepared for XPS analysis by distributing some of the powder on a circle of copper adhesive tape 6 mm in diameter so as to achieve uniform and complete coverage. The cellulose samples were also mounted on pieces of copper tape. Since these samples were non-conductive, it was necessary to use a low energy electron flood gun to neutralize charge. This causes peaks to shift to lower binding energy by approximately 4–6 eV. Two spots on each sample were analyzed and the surface compositions determined from the high resolution XPS spectra are representative of the compositions within the top ∼3 nm. Atom % by mass are reported with an uncertainty of $2\sigma = \pm4$%.

3. Results and discussion

3.1. Reaction conditions

The reaction conditions and abbreviations for the products are given in Table 1. Reactions were conducted in water, toluene, and DMF. Toluene and DMF were chosen because they readily dissolve the POSS monomers used. It was expected that DMF would produce a higher degree of POSS incorporation because DMF is known to swell cellulose; whereas the hydrophobic nature of toluene causes the cellulose structure to contract (Fidale, Ruiz, Heinze, & El Seoud, 2008). A high alkali concentration was used because this was found to maximize swelling in cellulose and facilitate a high product yield in the etherification of cellulose (Mansour, Basta, & Atwa, 1993). The

---

[1] The policy of NIST is to use metric units of measurement in all its publications, and to provide statements of uncertainty for all original measurements. In this document however, data from organizations outside NIST are shown, which may include measurements in non-metric units or measurements without uncertainty statements.

Table 1
Reaction conditions and abbreviations used for cellulose reactions.

Product identifier	Solvent	Cellulose modifier	Modifier: cellulose (w:w)	Product yield[a] (% by mass)
L040-6	None	none	0	n/a
PL040-6W	Water	GlyPh$_7$POSS	1:1	36.4
PL040-6D	DMF	GlyPh$_7$POSS	1:1	39.6
(1:1)PL040-6T	Toluene	GlyPh$_7$POSS	1:1	41.3
(2:3)PL040-6T	Toluene	GlyPh$_7$POSS	2:3	46.2
(1:3)PL040-6T	Toluene	GlyPh$_7$POSS	1:3	42.3
PGEL040-6T	Toluene	Phenyl glycidyl ether	5:1	17.0
SiL040-6T	Toluene	(EtO)$_2$(GlyOPr)MeSi	9:1	20.2
Ph8PL040-6T	Toluene	Ph$_8$POSS	1:1	44.0

[a] Product yield before soxhlet extraction to remove unbound modifier.

product yield of all reactions was quite low. Some of the loss was due to the alkalization process; as cellulose is well known to swell and partially dissolve in NaOH solutions (Nicoll, Cox, & Conaway, 1954). At 25 °C, the solubility of cellulose is quite low (<10% by mass); and we observed similar behavior in our samples. For the POSS reactions, analysis of the reaction filtrate indicated that most of the POSS remained in the solution and was not incorporated into the cellulose matrix. This was verified by elemental analysis of the cellulose product (see Section 3.2) and was the main cause of the low product yield. Washing the sodium cellulose with dry ethanol to remove excess aqueous NaOH prior to the reaction was found to have no effect on the product, POSS content, or product yield. This is in contrast with the phenyl glycidyl ether reactions examined by McKelvey et al. (1959); who found that the presence of some water was necessary to swell the cellulose and facilitate the reaction in toluene. It was found through FTIR and TGA analyses (see Section 3.4) that the final products required extensive washing to remove unbound residual POSS; so products were soxhlet extracted for 48 h using the same solvent as the reaction.

3.2. POSS content and degree of substitution

Presence of POSS in the product was examined using FTIR. (cf Fig. 1) We assign the main peaks in cellulose to –OH stretching as a broad peak between 3600 cm^{-1} and 3000 cm^{-1}, –CH stretching at 2900 cm^{-1}, –CH$_2$ bending at 1635 cm^{-1}, –CH bending at 1380 cm^{-1}, –C–O–C– stretching as a broad peak between 950 cm^{-1} and 1150 cm^{-1}, –CH$_2$ stretching at 900 cm^{-1}, and –OH bending at 685 cm^{-1}. (Lu, Askeland, & Drzal, 2008) Glycidyl phenyl POSS has characteristic peaks at 2900 cm^{-1} (C–H stretching), 1600 cm^{-1} (C=C stretching), 1430 cm^{-1} (C=C breathing), a broad peak between 1000 cm^{-1} and 1200 cm^{-1} (Si–O–Si stretching), and two peaks at 745 cm^{-1} and 695 cm^{-1} (=C–H bending). (Sulca et al., 2009; Zemke et al., 1996) The overlap of peaks around 3000 cm^{-1} and 1100 cm^{-1} make it difficult to assess either content or bonding within the product. However, peaks associated with the phenyl ring at 1600 cm^{-1}, 1430 cm^{-1}, 745 cm^{-1} and 695 cm^{-1} could be used to determine the presence of POSS in the product. Fig. 1b compares the FTIR between 1600 cm^{-1} and 600 cm^{-1} for better clarity. The low intensities suggest that very little POSS is incorporated in any product, with no evidence of POSS in the water and DMF reactions.

Degree of substitution (DS) of cellulose is typically reported as the number of substituted hydroxyls per glucose unit in the cellulose, with a maximum possible DS = 3. Using Si% by mass from elemental analysis, the DS for each reaction was calculated. (cf Table 2) The theoretical values were corrected for the presence of water as determined by TGA (see Section 3.4). Cellulose nanofibrils have a considerably higher surface area density compared to other forms of cellulose, which increases the available hydroxyl groups to surface modification (Siro & Plackett, 2010).

3.3. Fiber morphology and POSS distribution

The morphology of the nanofibrillated cellulose was examined using scanning electron microscopy. (cf Fig. 2) Although the use of water as the solvent did not result in a successful reaction, the SEM illustrates that the nanofibrillation was not affected by the harsh (high alkalinity and high temperature) reaction conditions. Likewise, reactions in toluene did not significantly change the degree of fibrillation in the cellulose. However, reactions in DMF resulted in the loss of nanofibrillation and some apparent fusion of the microfibers. Since Glycidyl Phenyl POSS is more readily soluble in DMF than toluene, it is likely that the POSS modified cellulose is partially dissolved in DMF during the reaction. The SEM also reveals the presence of small spheres when using toluene or DMF as the solvent. Energy dispersive X-ray microanalysis (EDS) indicted that these spheres are aggregated POSS crystals. As shown in Fig. 3,
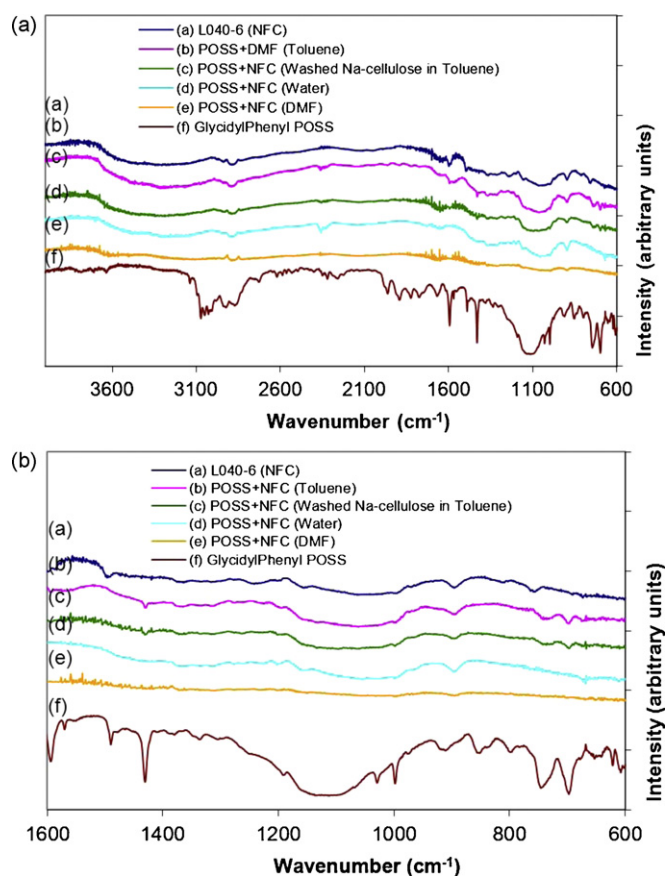

Fig. 1. FTIR-ATR of (a) cellulose products and (b) zoomed region identifying presence of GlyPh7POSS in the product. Plots have been shifted vertically for clarity.

Table 2
Elemental analysis of cellulose fibers modified using toluene.

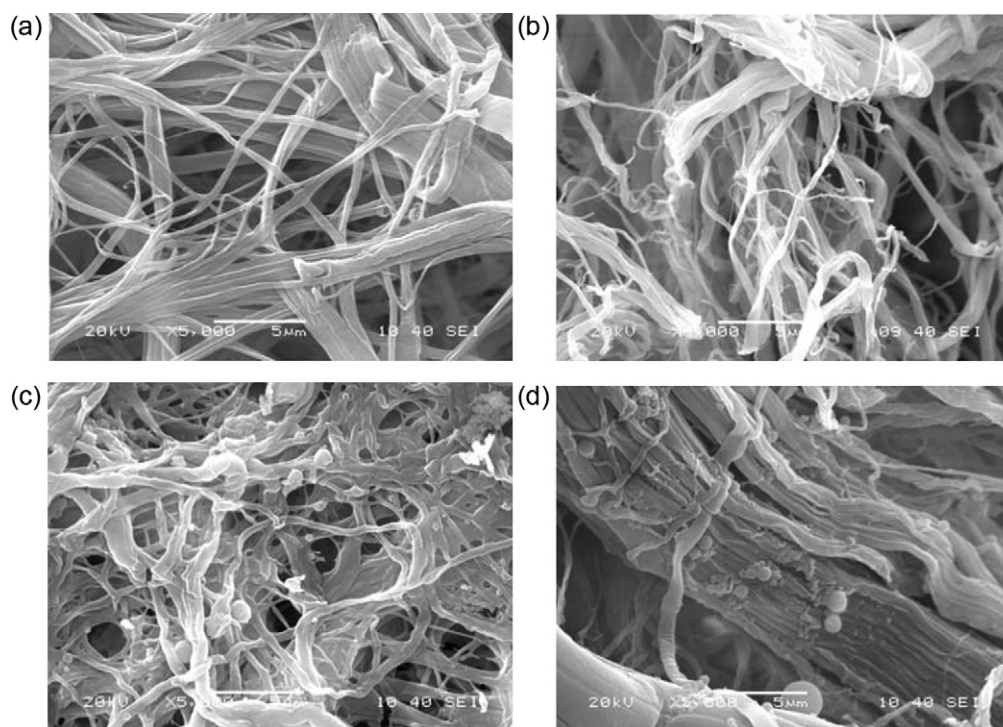| Cellulose fiber	Mass % C (theor.)	Mass % H (theor.)	Mass % Si (theor.)	DS
L040-6	41.6 (44.4)	6.4 (6.2)	–	–
(1:1)PL040-6T	40.9 (49.1)	6.3 (5.3)	1.8 (10.5)	0.11
(2:3)PL040-6T	41.7 (48.2)	6.2 (5.5)	2.7 (8.4)	0.18
(1:3)PL040-6T	41.0 (46.8)	6.3 (5.8)	0.9 (5.2)	0.05
PGEL040-6T	54.4 (66.7)	6.2 (5.8)	–	0.45
SiL040-6T	41.4 (52.7)	6.7 (8.6)	2.6 (9.5)	0.20
Ph8PL040-6T	39.0 (50.1)	6.4 (5.1)	0.9 (10.9)	0.05

Fig. 2. SEM of (a) L040-6, (b) PL040–6W, (c) (1:1)PL040-6T, and (d) PL040-6D.

after extraction with the solvent, these spheres were effectively removed.

3.4. Thermal properties and char yield

The thermal stability and char yield of the POSS-modified cellulose was determined using TGA under anaerobic conditions. (cf Fig. 4) The onset of degradation decreased and the char yield increased as the POSS content of the product increased. Based on char yields shown in Fig. 4a, POSS content in the product increased as the reaction solvent was changed from water to DMF to toluene. Elemental analysis indicated that the product contained approximately 10% POSS, so the 6-fold increase in char yield for PL0406-T indicates that POSS prevents some of the cellulose from decomposing.

TGA was also used to assess fiber purity and reaction efficiency. The as-received cellulose was found to contain some impurities which reduced thermal stability and increased char yield. It was
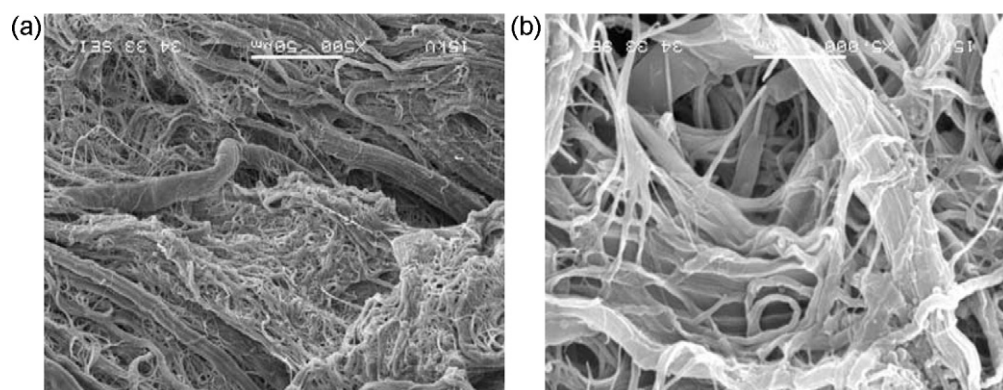

Fig. 3. SEM of (2:3)PL040-6T after soxhlet extraction in toluene at (a) low and (b) high magnification.

Table 3
PCFC data for modified cellulose fibers.

| Sample	HRC (W/g)	THR (kJ/g)	T_{peak} (°C)	Char (mass%)	TGA T_{peak}	TGA Char	Water (mass%)
Unmodified L0406	211	10.4	379	6.1	336	3.9	0.3
GlyPhPOSS	167	13.1	489	40.9	485	31.4	1.0
(1:1) GlyPhP-L0406	176	9.1	378	14.6	329	12.2	0.4
(2:3) GlyPhP-L0406	151	8.3	377	16.7	321	11.8	0.6
(1:3) GlyPhP-L0406	163	8.5	378	12.2	332	4.0	1.7
(1:1) Ph8P-L0406	165	8.6	375	11.6	335	9.8	0.3
PGEL0406-T	254	17.5	388	17.2	341	12.7	0.5
SiL0406-T	48	7.4	317	23.6	273	22.3	0.8
SiL0406-T washed	179	12.7	386	6.6	365	5.2	0.7
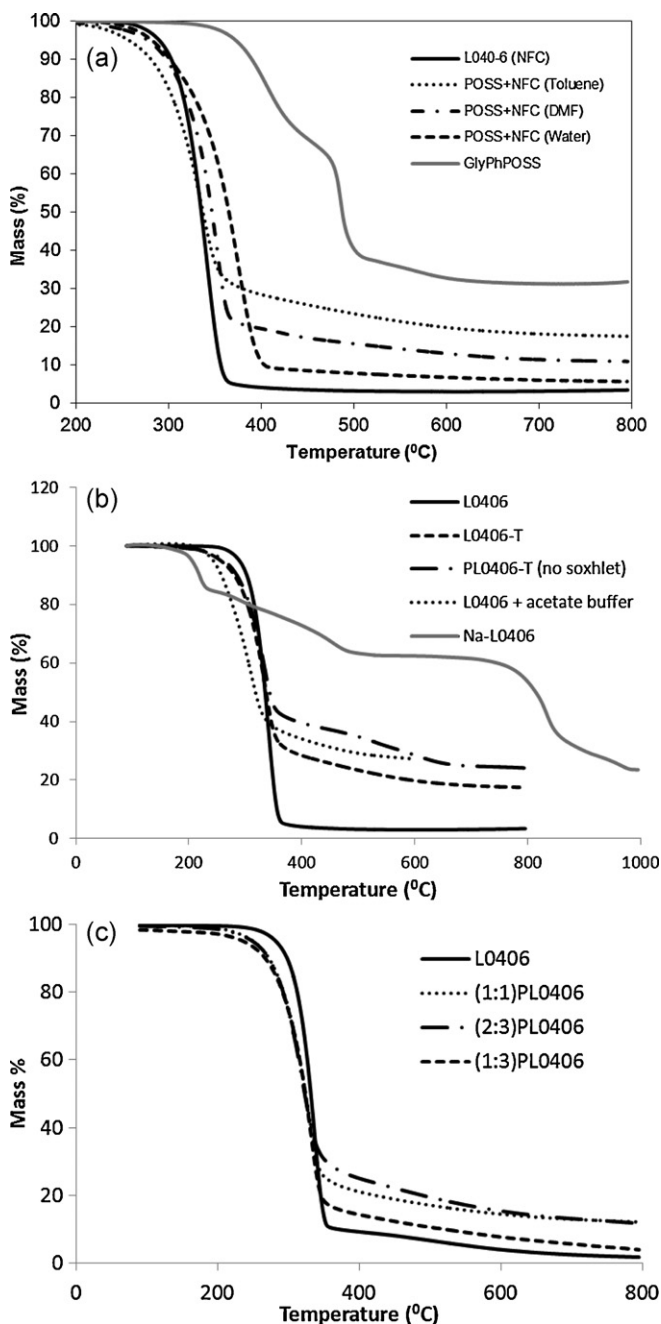
Fig. 4. Effects of (a) reaction solvent (b) product impurities, and (c) POSS:cellulose reaction ratio on the thermal stability of PL040-6 at a scan rate of 10 °C/min under a flow of 60 mL/min nitrogen.

found that washing the cellulose in dilute acetic acid followed by water effectively removed the impurities and produced fibers with thermal stabilities about 10 °C higher than microcrystalline cellulose. Incomplete washing of the cellulose or final product would leave some sodium or acetate ions in the fibers. As shown in Fig. 4b, either of these would result in a significant decrease in thermal stability and an increase in char yield. As noted in Section 3.3, without soxhlet extraction of the fibers, unreacted POSS aggregates into small spheres on the fiber. The excess POSS results in a higher char yield, but does not affect the thermal stability. The effects of POSS:cellulose reactant ratios and DS on the thermal stability and char yield are shown in Fig. 4c. The initial loss in mass below 100 °C is due to adsorbed water and was used to determine the water content of the fibers. It was found that the dried cellulose picks up water from the air within 15 min and the equilibrium amount of moisture pick-up is about 1% by mass. The char yields and water contents are included in Table 3.

TGA on its own is not a good indicator of flammability. PCFC can provide some evidence of material performance in a fire. We sent samples to the University of Dayton Research Institute for analysis. The results of their tests are shown in Table 3.

The heat release capacity (HRC) from PCFC analyses correlates very well with heat release rates from cone calorimetry, LOI values, and UL94 ratings. Modifying cellulose with POSS results in a 25–30% decrease in HRC and a 3-fold increase in char yield. This is significantly better than an average of pure cellulose and pure POSS. The slight increase in heat release and decrease in char yield for (1:1) GlyPhP-L0406 is consistent with the lower DS observed for this product. Silane modified cellulose initially appeared to produce the best PCFC results. However, XPS data (see Section 3.5) indicated the presence of Na^+ impurity due to incomplete washing. After rewashing, the HRC rose to values comparable with our POSS modified samples. The higher THR and lower char yield show that the silane treated cellulose is not as well protected as using POSS compounds.

3.5. Char analysis

To assess the usefulness of the char formed during pyrolysis, scanning electron microscopy (SEM) coupled with electron dispersion spectroscopy (EDS) was used to assess the morphology and surface composition of the chars formed during TGA pyrolysis under nitrogen. In addition, samples were analyzed for additional surface analysis of the chars using X-ray photoelectron spectroscopy (XPS). SEM images of (2:3) GlyPhP-L0406 and its char are shown in Fig. 5 and SEM images of (1:1) Si-L0406 and its char are shown in Fig. 6. The elemental composition of the fibers and chars using elemental analysis, EDS, and XPS are shown in Table 4.

One of the striking features of the POSS modified cellulose chars is that the nanofibrillated structure remains intact. Indeed, it is difficult to differentiate between the modified fibers and their chars. Some images of the modified cellulose indicate the presence of some excess POSS as a powdery matte trapped between the
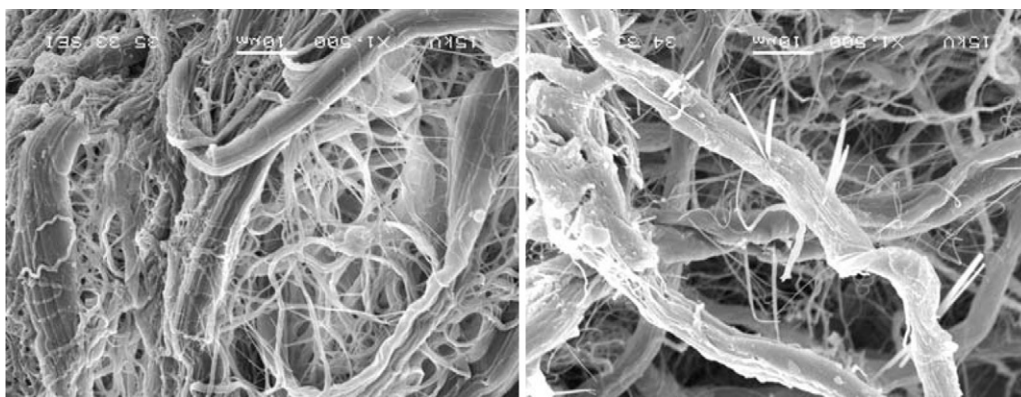
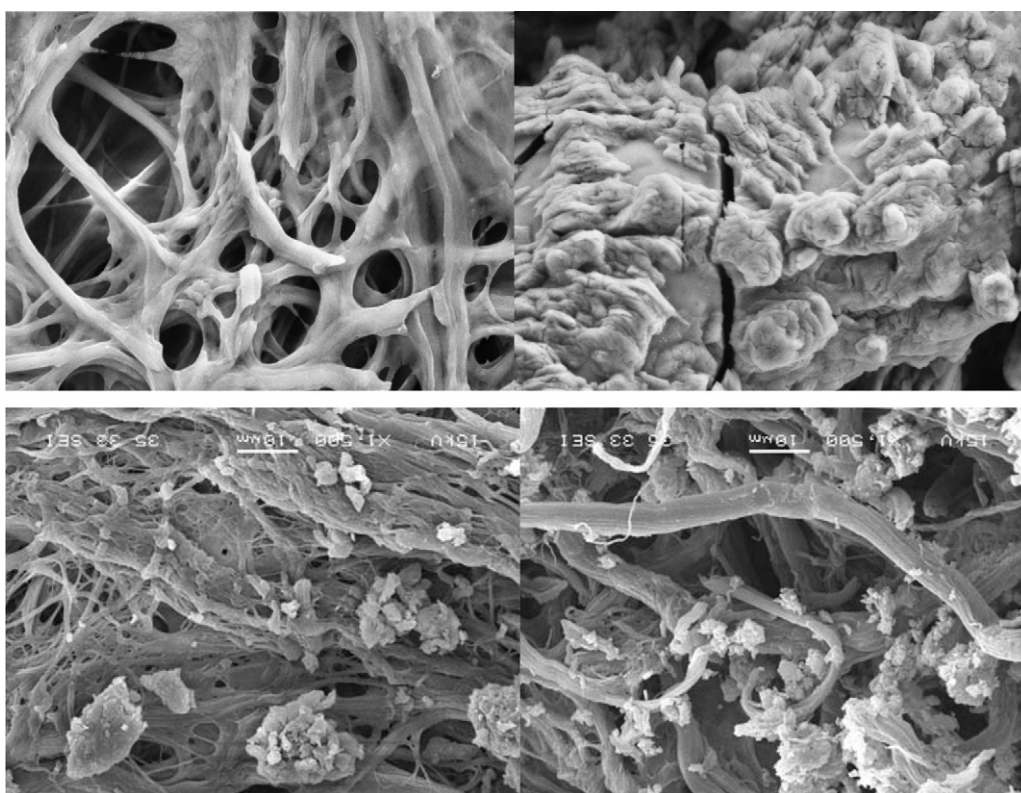**Fig. 5.** SEM images of (2:3) PhGlyP-L0406 (left) and its char (right) at high magnification.

Fig. 6. SEM images of (1:1) Si-L0406 (left) and its char (right) before (top) and after (bottom) washing at high magnification.

Table 4
Elemental composition of modified cellulose and their chars.

Sample	Test	H	C	O	Si	Na
L0406	EA	6.4	41.7	52		
GlyPhP	EA	4.3	53.8	21	21.0	
	XPS		60.8	25.4	13.8	
GlyPhP Char	XPS		26.4	52.8	20.9	
(2:3)PL0406-T	EA	6.1	43.9	47	1–4	
	EDS		76.4	19.5	2.0	2.0
	XPS		85.1	11.7	3.2	<0.1
(2:3)PL0406-T	EDS		23.7	50.9	23.4	2.0
Char	XPS		17.1	49.5	10.0	0.6
SiL0406-T	EA	6.2	54.7	33	2.7	
	EDS		70.9	21.8	3.8	3.4
	XPS		57.5	37.5	3.9	1.2
SiL0406-T	EDS		13.5	46.7	4.6	35.2
Char	XPS		17.1	49.5	10.0	23.6
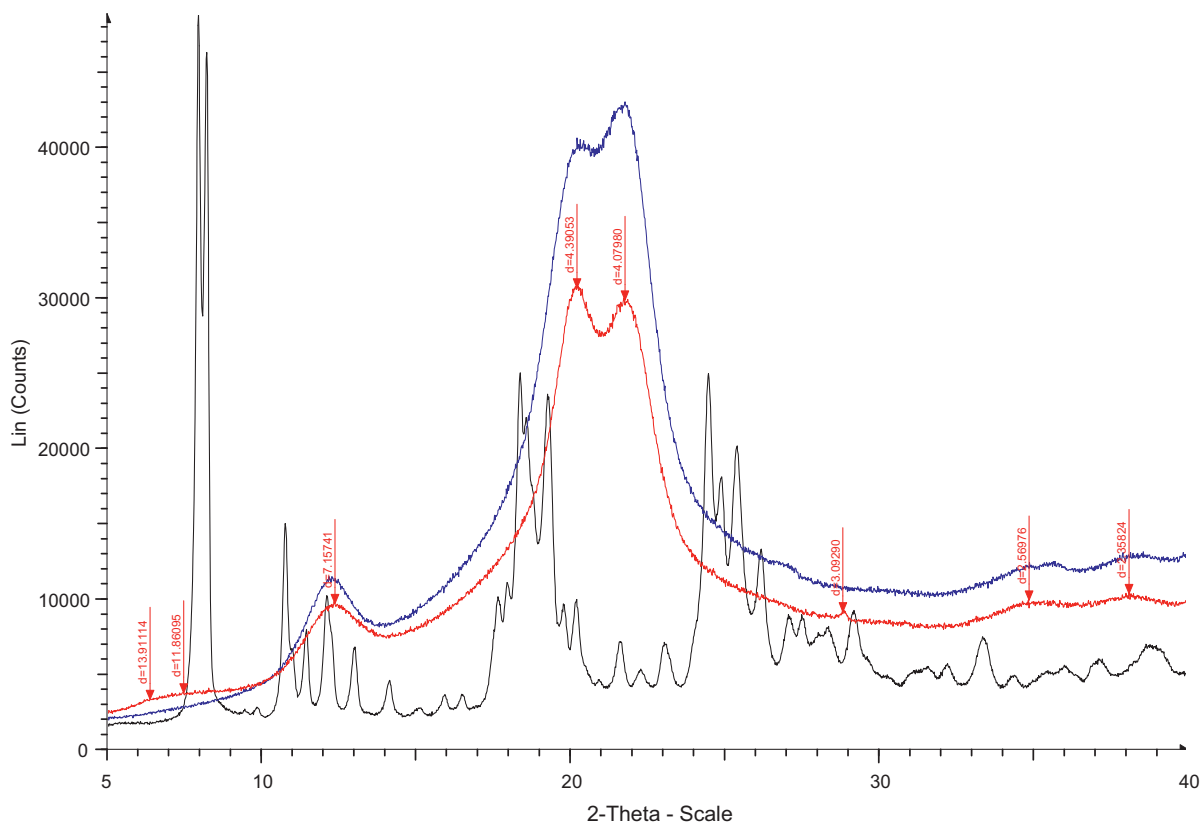
OctPhPOSS - File: OctPhPOSS.raw - Type: Locked Coupled - Start: 5.000 ° - End: 39.995 ° - Step: 0.017 ° - Step time: 273.9 s - Temp.: 25 °C (Room) - Time Started: 9 s - 2-Theta: 5.000 ° - Theta: 2.50
Operations: Import

POSS-L040-6 - File: POSS-L040-6.raw - Type: Locked Coupled - Start: 5.000 ° - End: 39.995 ° - Step: 0.017 ° - Step time: 273.9 s - Temp.: 25 °C (Room) - Time Started: 17 s - 2-Theta: 5.000 ° - Theta:
Operations: Import

Lo40-6-WaAshed-pressed - File: Lo40-6-WaAshed-pressed.raw - Type: 2Th/Th locked - Start: 5.000 ° - End: 39.995 ° - Step: 0.017 ° - Step time: 273.9 s - Temp.: 25 °C (Room) - Time Started: 17 s - 2-
Operations: Import

Fig. 7. Powder X-ray diffraction of cellulose fibers as received and after POSS modification.

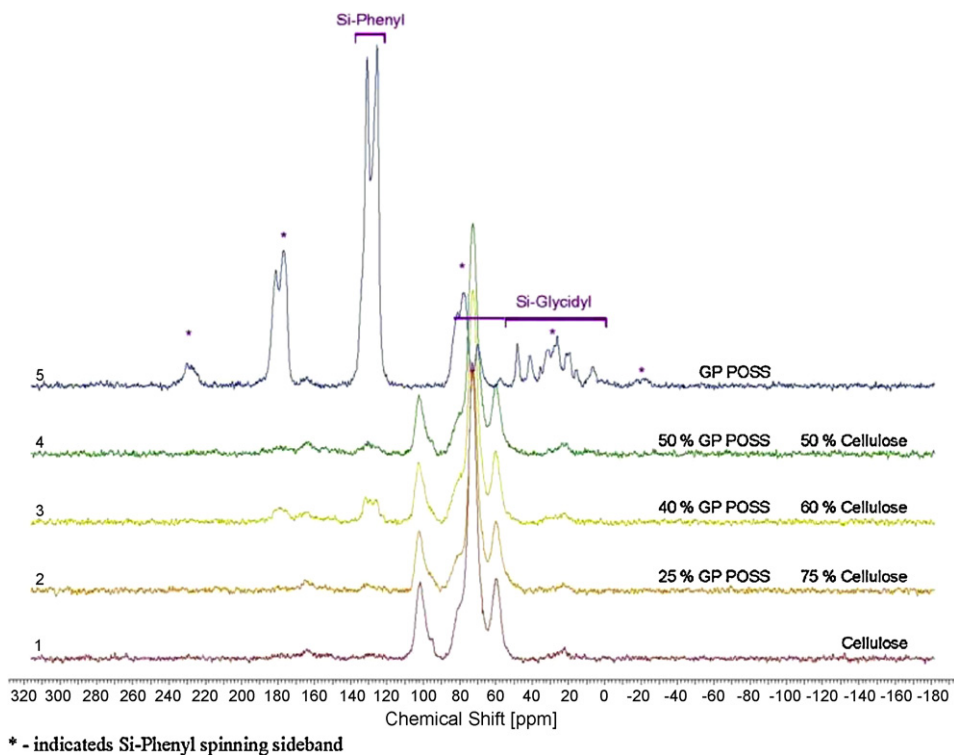

* - indicateds Si-Phenyl spinning sideband

Fig. 8. ^{13}C MAS-NMR of (a) L040-6, (b) GlyPh7POSS, (c) (1:1)PL040-6T, (d) (2:3)PL040-6T, and (1:3)PL040-6T.
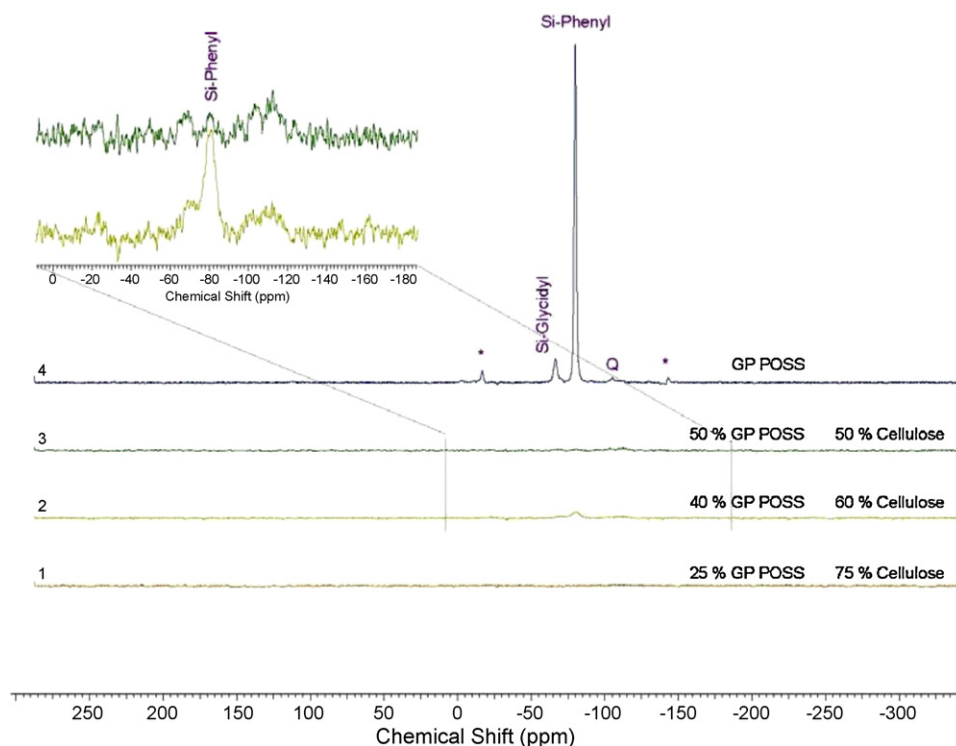
Fig. 9. ^{29}Si MAS-NMR of (a) L040-6, (b) GlyPh7POSS, (c) (1:1)PL040-6T, (d) (2:3)PL040-6T, and(1:3)PL040-6T. Inset shows an enlargement in the region associated with Si–Phenyl bonds.

nanofibrillated ends (image not shown). However, the majority of samples examined show little difference between the unmodified cellulose and modified cellulose other than some minor fraying of the fibrils. In contrast, the silane modified fibers (Fig. 6) reveal a plasticizing or cross-linking effect during the modification process. Rewashing the fibers resulted in the loss of some of this effect, but left crystals on the fiber surface. In addition, the cellulose remains largely unprotected during pyrolysis, resulting in a nearly complete loss of fibrillation and a coarse deposit of char along the surface of the larger fibers. The pyrolysis can also result in the formation of needle-like or crystalline formations (image not shown). The XPS and EDS results indicate a high level of Na and CO_3, which may indicate that the excess Na^+ crystallizes with cellulosic char precursors to form Na_2CO_3 particles on the surface.

The elemental composition of the reactants and modified cellulose fibers were characterized using elemental analysis (EA) and XPS. The chars were characterized using XPS and EDS. For most of the samples, the results from EDS correlate very well with XPS. XPS of pure cellulose has been shown to correlate very well with elemental analysis (Cunha et al., 2010) indicating a homogeneous structure. Four key features are evident from the analyses shown in Table 4: (1) The POSS modified cellulose shows a surface composition that is poorer in oxygen and richer in carbon and silicon, indicating that the POSS effectively and fairly uniformly surrounds the cellulose. (2) The charred surface is predominantly a form of silicon oxide, suggesting a ceramic-like protective layer formed during decomposition. (3) The silane treated cellulose has a surface composition similar to the bulk composition illustrating that the silane cannot separate or protect the cellulose fibers very well. (4) The char of the silane treated cellulose has a very high Na^+ content, indicating incomplete washing of the final product. Since alkali metals are known to catalyze pyrolysis, leading to lower thermal stabilities and significant char formation, the PCFC results for (1:1) Si-L0406 is likely due to the high Na^+ content of the fibers. This also indicates that much of the silane coupling agent may have cross-linked

with itself and is physically adsorbed to the surface of the cellulose rather than covalently bonded, similar to findings of other authors (Matuana et al., 1999; Abdelmouleh et al., 2002; Cunha et al., 2010).

3.6. Cellulose–POSS binding

POSS monomers tend to aggregate and bound POSS often self-assemble in systems where the POSS organic substituents have poor compatibility with the tethered compound. This typically results in POSS-rich crystalline domains exhibiting sharp peaks in powder X-ray diffraction patterns. As illustrated in Fig. 7 powder X-ray diffraction revealed the loss of POSS crystalline domains after the reaction. Although this could be due to the low reaction efficiency noted earlier, it could also be an indication of side reactions that destroy the Si–O cage structure.

To help determine (a) whether POSS is covalently bonded to the cellulose surface or just physically trapped by the nanofibrils and (b) if the harsh basic conditions of the reaction results in POSS cage opening, we examined the solid state NMR of the cellulose products. The glycidyl peaks in the ^{13}C MAS NMR (cf Fig. 8) were too low to determine whether the POSS–cellulose interactions were physical or chemical in nature. However, the TGA and coagulation in ethanol solutions (cf Fig. 3) strongly suggest there is at least some chemical bonding in these systems.

The ^{29}Si MAS NMR (cf Fig. 9) shows some peak broadening and a potential peak at 110 ppm, indicative of $SiO_{4/2}$. In addition, the XRD of the POSS modified cellulose (cf Fig. 7) further suggests that the POSS cage is opening in the basic reaction conditions, reducing characteristic POSS–POSS crystalline peaks. Finally, a recent reaction of $Ph_8POSS + L0406$ without sodium hydroxide under the same reaction conditions resulted in no POSS residue after the reaction as indicated by EA, TGA, and FTIR. This confirms the opening of the POSS cage and strong interactions between the resulting silanol groups and the hydroxyl groups on the cellulose surface.
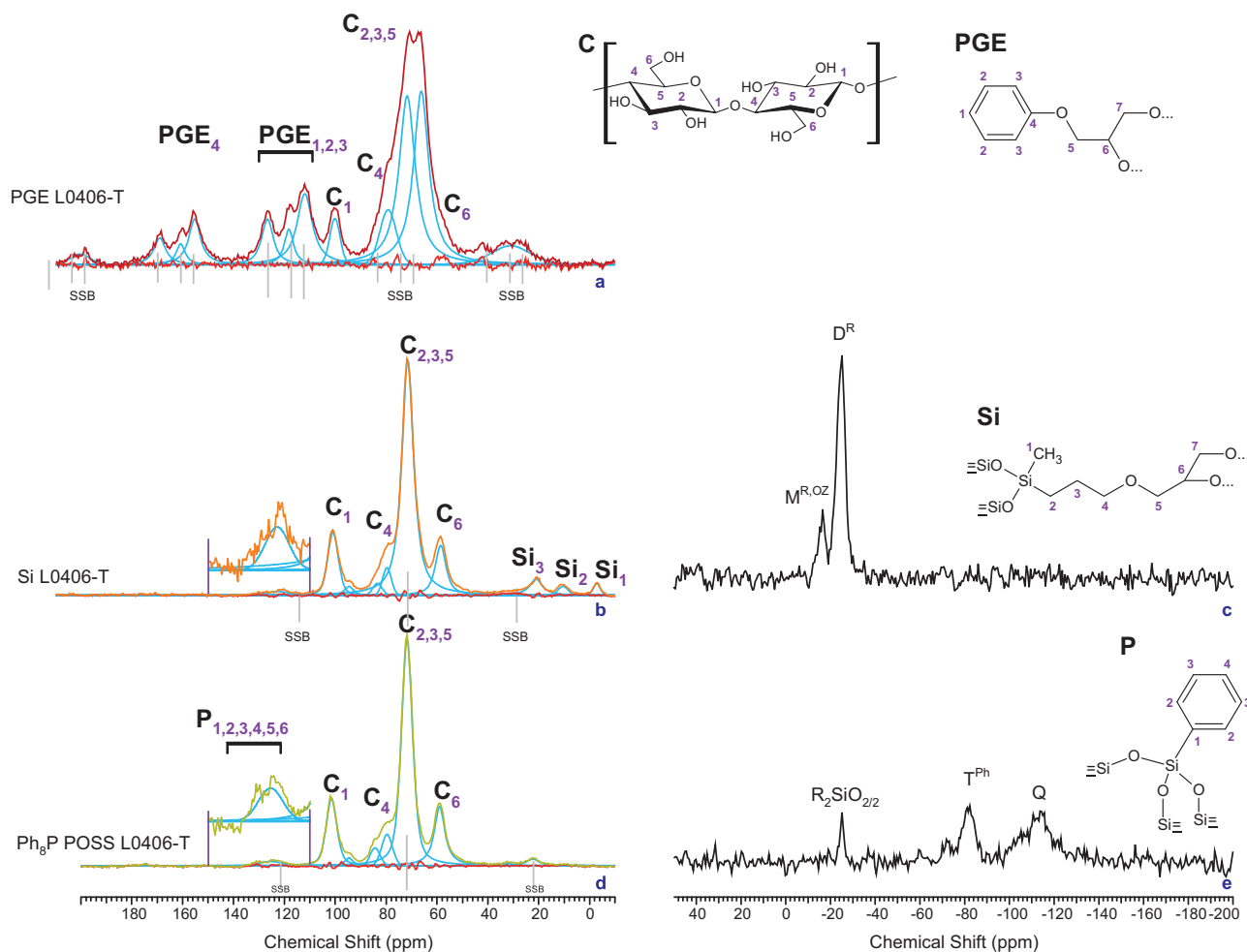
Fig. 10. ^{13}C and ^{29}Si NMR using the CPMAS and MAS methods for cellulose control samples, PGEL0406-T, Si-L0406-T, and Ph8P-L0406-T, conducted by our collaborators at Dow Corning.

Due to the low signal to noise ratio of the POSS modified cellulose, it was difficult to determine with certainty whether the POSS had covalently bonded to the cellulose or was physically adsorbed or trapped in the nanofibrillar structure. To confirm the results, we also analyzed the control samples of phenyl glycidyl ether modified cellulose, diethoxy(3-glycidyloxypropyl)methylsilane modified cellulose, and OctaPhenylPOSS modified using solid state ^{13}C and ^{29}Si analysis. The results (shown in Fig. 10) helped clarify whether or not there was covalent bonding to the cellulose as well as whether or not the POSS cage is opening and/or hydrolyzing due to the harsh reaction conditions. All samples clearly demonstrate the presence of cellulose. Consumption of glycidyl epoxy groups is demonstrated by the absence of epoxy functional carbons in the ^{13}C NMR results. In both cases, the glycidyl functional materials show good correlation to the anticipated ether products resulting from the epoxy groups bridging active cellulose sites. Additionally, in the case of the dialkoxysilane, it is noted that the primary silane product is transformed to the hydrolysis and condensation product $(Me,R)SiO_{2/2}$ with a minor product of $(Me,R)SiO_{1/2}OZ$, where Z may be H or cellulose and R is propylglycidoxy. This indicates preferential siloxane type polymer growth and significantly reduces effective silanation of the cellulose. Finally, Ph8POSS is observed to be present at low concentrations in the Ph8L0406-T sample. However, a significant portion of the silicon species observed in this sample indicates the oxidation of the Ph8POSS group to produce $SiO_{4/2}$. Since this last sample did

not contain any glycidyl reactive groups, the results verify that a significant portion of the POSS cage is opening and that binding between the oxygens of the opened cage and cellulose can occur. Some coupling of the opened POSS cages occurs as a side product and either strongly physisorbs on the cellulose nanofibrils or chemisorbs through one of the other exposed oxygens of the POSS cage.

Strong binding between the POSS and cellulose were confirmed by dispersing the fibers in a 50% by mass aqueous ethanol solution. As shown in Fig. 11, pure cellulose swells and forms a stable suspension in the solution, whereas the POSS modified cellulose does not mix in the solvent. This illustrates the increase in hydrophobicity upon incorporation of the phenyl decorated POSS into the cellulose matrix. As with the NMR results, this strongly suggests covalent bonding occurred during the reaction.

Although these results show that the POSS materials do not bind solely through the glycidyl groups, it also illustrates an advantage to use the more expensive POSS reactant over more readily obtainable silane reagents. The rich supply of oxygens and bulkiness of the POSS cage favor covalent binding to the cellulose over polymerized ether products such as those found when using glycidyl functionalized silanes. The opening of the POSS cage is not necessarily disadvantageous, as a number of authors have shown the usefulness of combining trisilanol POSS monomers in improving mechanical and thermal properties of polymers (Misra et al., 2009; Zhao & Schiraldi, 2005). Since the trisilanol POSS is known

Fig. 11. L040-6 (left) and PL0406-T (right) mixed in 50% by mass ethanol–water solutions.

to decompose around 280 °C, the slight decrease in thermal stability noted in Section 3.4 for POSS-modified cellulose may be due to decomposition of the destroyed POSS cages (Zeng et al., 2005). We are currently examining the effectiveness of the POSS-modified cellulose as a flame retardant additive in poly(lactic acid).

4. Conclusions

We successfully modified nanofibrillated cellulose with GlycidylPhenyl POSS. The largest amount of POSS was incorporated using toluene as a solvent, and adding more POSS than a 2:3 POSS:cellulose ratio did not increase the content of POSS in the final product. The highest amount of POSS was found to be 10 mass%, which corresponds to DS = 0.05. The modified cellulose was found to protect the underlying cellulose from complete degradation and produce greater than a 5-fold increase in char under anaerobic conditions with a minimal decrease in thermal stability. SEM images show that the nanofibrillated structure was retained, even after thermal degradation. In addition, excess POSS aggregates in small spheres distributed fairly evenly along the cellulose surface unless the fibers are thoroughly washed in the reaction solvent. Elemental analysis and XPS indicates that modified cellulose surface is decorated with the phenyl groups on the POSS, that the char surface is predominantly silicon oxide, and that the silane treated cellulose cannot protect the cellulose as well as POSS. The POSS treatment increased the hydrophobic nature of the cellulose. Solid state NMR spectra, TGA, and solubility behavior reveal that some of the POSS is covalently bonded to the cellulose, but that the Si-O cage structure was damaged during the reaction. There is also some evidence of POSS coupling and interactions between the exposed cage oxygens and the hydroxyl groups on the cellulose. Silane treated cellulose is dominated by physical adsorption of the silane coupling agent at the surface of the cellulose. Despite the inability to retain the POSS structure during the reaction, the simple two-step, one-pot process with low toxicity and previously reported benefits of the POSS-cellulose species formed clearly show the merits to our approach. The use of the modified cellulose in intumescing flame retardant formulations for polymers is currently under investigation.

References

Abdelmouleh, M., Boufi, S., Salah, A. B., Belgacem, M. N., & Gandini, A. (2002). Interaction of silane coupling agents with cellulose. *Langmuir*, 18, 3203–3208.

Anna, P., Marosi, Gy., Bertalan, Gy., Marton, A., & Szep, A. (2002). Structure–property relationship in flame retardant polymers. *Journal of Macromolecular Science B: Physics*, B41, 1321–1330.

Antal, M. J., Jr., & Varhegyi, G. (1995). Cellulose pyrolysis kinetics: The current state of knowledge. *Industrial and Engineering Chemistry Research*, 34, 703–717.

Blasi, C. D. (2008). Modeling chemical and physical processes of wood and biomass pyrolysis. *Progress in Energy and Combustion Science*, 34, 47–90.

Bourgibot, S., Duquesne, S., & Jama, C. (2006). Polymer nanocomposites: How to reach low flammability? *Macromolecular Symposium*, 233, 180–190.

Cardoen, G., & Coughlin, E. B. (2004). Hemi-telechelic polystyrene-POSS copolymers as model systems for the study of well-defined inorganic/organic hybrid materials. *Macromolecules*, 37, 5123–5126.

Chigwada, G., Jash, P., Jiang, D. D., & Wilkie, C. A. (2005). Fire retardancy of vinyl ester nanocomposites: Synergy with phosphorus–based fire retardants. *Polymer Degradation and Stability*, 89, 85–100.

Clemons, C. M., Caulfield, D. F., & Giacomin, A. F. (1999). Dynamic fracture toughness of cellulose-fiber-reinforced polypropylene: Preliminary investigation of microstructural effects. *Journal of Elastomers and Plastics*, 31, 367–378.

Cunha, A. G., Freire, C., Silvestre, A., Neto, C. P., Gandini, A., Belgacem, M. N., Chaussy, D., & Beneventi, D. (2010). Preparation of highly hydrophobic and lipophobic cellulose fibers by a straightforward gas–solid reaction. *Journal of Colloid and Interface Science*, 344, 588–595.

Fidale, L. C., Ruiz, N., Heinze, T., & El Seoud, O. A. (2008). Cellulose swelling by aprotic and protic solvents: What are the similarities and differences? *Macromolecular Chemistry and Physics*, 209, 1240–1254.

Fina, A., Tabuani, D., Frache, A., & Camino, G. (2005). Polypropylene–polyhedral oligomeric silsesquioxanes (POSS) nanocomposites. *Polymer*, 46, 7855–7866.

Fina, A., Abbenhuis, H. C. L., Tabuani, D., & Camino, G. (2006). Metal functionalized POSS as fire retardants in polypropylene. *Polymer Degradation and Stability*, 91, 2275–2281.

Fox, D. M., Maupin, P. H., Bellayer, S., Murariu, M., Harris, R. H., Jr., Gilman, J. W., Eldred, D. V., Katsoulis, D., Trulove, P. C., & De Long, H. C. (2007). Use of a polyhedral oliomeric silsesquioxane (POSS)–imidazolium cation as an organic modifier for montmorillonite. *Langmuir*, 23, 7707–7714.

Fox, D. M., Lee, J., Ford, E., Balsley, E., Zammarano, M., Matko, S., & Gilman, J. W. (2010). POSS-modified cellulose for improving flammability characteristics of polystyrene. In *10th International Conference on Wood & Biofiber Plastic Composites* Madison, Wisconsin: Forest Products Society, (pp. 337–342).

Fox, D. M., Lee, J., Jones, J. M., Zammarano, M., & Gilman, J. W. (2010). Microencapsulated POSS in cellulose using 1-ethyl-3-methylimidazolium acetate. *ECS Transactions*, 33, 99–108.

Fox, D. M., Harris, R. H., Jr., Bellayer, S., Gilman, J. W., Gelfer, M. Y., Hsaio, B. S., Maupin, P. H., Trulove, P. C., & De Long, H. C. (2011). The Pillaring Effect of the 1,2-Dimethyl-3(benzyl ethyl iso-butyl POSS) imidazolium Cation in Polymer/Montmorillonite Nanocomposites. *Polymer*, 52, 5335–5343.

Franchini, E., Galy, J., Gerard, J.-F., Tabuani, D., & Medici, A. (2009). Influence of POSS structure on the fire retardant properties of epoxy hybrid networks. *Polymer Degradation and Stability*, 94, 1728–1736.

Gerard, C., Fontaine, G., & Bourbigot, S. (2011). Synergistic and antagonistic effects in flame retardancy of an intumescent epoxy. *Polymers for Advanced Technologies*, 22, 1085–1090.

Girones, J., Pimenta, M. T. B., Vilaseca, F., de Carvalho, A. J. F., Mutje, P., & Curvelo, A. A. S. (2007). Blocked isocyanates as coupling agents for cellulose-based composites. *Carbohydrate Polymers*, 68, 537–543.

Jiao, Y.-H., Wang, X.-L., Wang, Y.-Z., Wang, D.-Y., Zhai, Y.-L., & Lin, J.-S. (2009). Thermaldegradation and combustion behaviors of flame-retardant polypropylene/thermoplastic polyurethane blends. *Journal of Macromolecular Science B Physics*, 48, 889–909.

Jonoobi, M., Harun, J., Matthew, A. P., & Oksman, K. (2010). Mechanical properties of cellulose nanofiber (CNF) reinforced polylatic acid (PLA) prepared by twin screw extrusion. *Composites Science and Technology*, *70*, 1742–1747.

Joseph, K., Thomas, S., & Pavithran, C. (1996). Effect of chemical treatment on the tensile properties of short sisal fibre-reinforced polyethylene composites. *Polymer*, *37*, 5139–5149.

Khelfa, A., Finqueneisel, G., Auber, M., & Weber, J. V. (2008). Influence of some minerals on the cellulose thermal degradation mechanisms: Thermogravimetric and pyrolysis-mass spectrometry studies. *Journal of Thermal Analysis and Calorimetry*, *92*, 795–799.

Li, B., & He, J. (2004). Investigation of mechanical property, flame retardancy and thermal degradation of LLDPE-wood-fibre composites. *Polymer Degradation and Stability*, *83*, 241–246.

Li, G., Wang, L., Ni, H., & Pittman, C. U., Jr. (2001). Polyhedral oligomeric silsesquioxane (POSS) polymers and copolymers (a review). *Journal of Inorganic and Organometallic Polymers*, *11*, 123–154.

Liu, L., Hu, Y., Song, L., Nazare, S., He, S., & Hull, R. (2007). Combustion and thermal properties of OctaTMA-POSS/PS composites. *Journal of Materials Science*, *42*, 4325–4333.

Liu, L., Hu, Y., Song, L., Gu, X., & Ni, Z. (2010). Preparation, characterization and properties of polystyrene composites using octaphenyl polyhedral oligomeric silsesquioxane and its bromide derivative. *Iranian Polymer Journal*, *19*, 937–948.

Ljungberg, N., Bonini, C., Bortolussi, F., Boisson, C., Heux, L., & Cavaille, J. Y. (2005). New nanocomposite materials reinforced with cellulose whiskers in atactic polypropylene: Effect of surface and dispersion characteristics. *Biomacromolecules*, *6*, 2732–2739.

Lu, J., Askeland, P., & Drzal, L. T. (2008). Surface modification of microfibrillated cellulose for epoxy composite applications. *Polymer*, *49*, 1285–1296.

Mansour, O. Y., Basta, A. H., & Atwa, A. I. (1993). Hydroxyethyl cellulose I. Variables affecting the hydroxyethylation reaction. *Polymer: Plastics Technology and Engineering*, *32*, 415–430.

Matuana, L. M., Balatinecz, J. J., Park, C. B., & Sodhi, R. N. S. (1999). X-ray photoelectron spectroscopy study of silane-treated newsprint-fibers. *Wood Science and Technology*, *33*, 259–270.

McCusker, C., Carroll, J. B., & Rotello, V. M. (2005). Cationic polyhedral oligomeric silsesquioxane (POSS) units as carriers for drug delivery processes. *Chemical Communications*, 996–998.

McKelvey, J. B., Webre, B. G., & Klein, E. (1959). Reaction of epoxides with cotton cellulose in the presence of sodium hydroxide. *Textile Research Journal*, *29*, 918–925.

Misra, R., Alidedeoglu, A. H., Jarrett, W. L., & Morgan, S. E. (2009). Molecular miscibility and chain dynamics in POSS/polystyrene blends: Control of POSS preferential dispersion states. *Polymer*, *50*, 2906–2918.

Nicoll, W. D., Cox, N. L., & Conaway, R. F. (1954). IX. Derivatives of cellulose. D. Alkali and other metal derivatives. In E. Ott, H. M. Spurlin, & M. W. Grafflin (Eds.), *Cellulose and cellulose derivatives* (2nd ed., pp. 825–881). New York: Interscence Publishers Inc.

Phillips, S. H., Haddad, T. S., & Tomczak, S. J. (2004). Developments in nanoscience: Polyhedral oligomeric silsequioxane (POSS)–polymers. *Current Opinion in Solid State and Materials Science*, *8*, 21–29.

Qian, Y., Wei, P., Zhao, X., Jiang, P., & Yu, H. Flame retardancy and thermal stability of polyhedral oligomeric silsesquioxane nanocomposites, Fire and Materials, in press.

Ramiah, M. V. (1970). Thermogravimetric and differential thermal analysis of cellulose, hemicelluloses, and lignin. *Journal of Applied Polymer Science*, *14*, 1323–1337.

Roman, M., & Winter, W. T. (2004). Effect of sulfate groups from sulfuric acid hydrolysis on the thermal degradation behavior of bacterial cellulose. *Biomacromolecules*, *5*, 1671–1677.

Saddawi, A., Jones, J. M., Williams, A., & Wojtowicz, M. A. (2010). Kinetics of the thermal decomposition of biomass. *Energy & Fuels*, *24*, 1274–1282.

Samir, M. A. S. A., Alloin, F., & Dufresne, A. (2005). Review of recent research into cellulosic whiskers, their properties and their application in nanocomposite field. *Biomacromolecules*, *6*, 612–626.

Schwab, J. J., & Lichtenhan, J. D. (1998). Polyhedral oligomeric silsesquioxane (POSS)-based polymers. *Applied Organometallic Chemistry*, *12*, 707–713.

Shimada, N., Kawamoto, H., & Saka, S. (2008). Different action of alkali/alkaline earth metal chlorides on cellulose pyrolysis. *Journal of Analytical and Applied Pyrolysis*, *81*, 80–87.

Siro, I., & Plackett, D. (2010). Microfibrillated cellulose and new nanocomposite materials: A review. *Cellulose*, *17*, 459–494.

Sulca, N. M., Lungu, A., Popescu, R., Garea, S. A., & Iovu, H. (2009). New polymeric nanocomposites based on polyhedral oligomeric silsesquioxanes. *Materiale Plastice*, *46*, 1–10.

Tajvidi, M., Feizmand, M., Falk, R. H., & Felton, C. (2009). Effect of cellulose fiber reinforcement on the temperature dependent mechanical performance of Nylon 6. *Journal of Reinforced Plastics and Composites*, *28*, 2781–2790.

Tang, W. K., Eickner, H. W. (1968) Effect of inorganic salts on pyrolysis of wood, cellulose, and lignin determined by differential thermal analysis. *U.S. Forest Service Research Paper FPL 82*, U.S. Department of Agriculture, Madison, WI, 1–30.

Vannier, A., Duquesne, S., Bourbigot, S., Castrovinci, A., Camino, G., & Delobel, R. (2008). The use of POSS as a synergist in intumescent recycled poly(ethylene terephthalate). *Polymer Degradation and Stability*, *93*, 818–826.

Wanna, J. T., & Powell, J. E. (1993). Thermal decomposition of cotton cellulose treated with selected salts. *Thermochimica Acta*, *226*, 257–263.

Weil, E. D., & Levchik, S. V. (2008). Flame retardants in commercial use or developments for textiles. *Journal of Fire Sciences*, *26*, 243–281.

Wu, J., Yu, D., Chan, C.-M., Kim, J., & Mai, Y.-W. (2000). Effect of fiber pretreatment condition on the interfacial strength and mechanical properties of wood fiber/PP composites. *Journal of Applied Polymer Science*, *76*, 1000–1010.

Wu, J., Haddad, T. S., Kim, G. M., & Mather, P. T. (2007). Rheological behavior of entangled polystyrene-polyhedral oligosilsesquioxane (POSS) copolymers. *Macromolecules*, *40*, 544–554.

Wu, J., Haddad, T. S., & Mather, P. T. (2009). The role of vertex group in rheological behavior of entangled polystyrene-polyhedral oligosilsesquioxane (POSS) copolymers. *Macromolecules*, *42*, 1142.

Yang, H., Yan, R., Chen, H., Lee, D.-H., & Zheng, C. (2007). Characteristics of hemicelluloses, cellulose, and lignin pyrolysis. *Fuel*, *86*, 1781–1788.

Zemke, G. W., Moro, J. R., Gomez-Pineda, E. A., & Winkler-Hechenleitner, A. A. (1996). Benzylcellulose from a cotton residue cellulose: Characterization by thermal analysis and infrared spectroscopy. *International Journal of Polymeric Materials*, *34*, 197–210.

Zeng, J., Bennett, C., Jerret, W. L., Iyer, S., Kumar, S., Mathias, L. J., & Schiraldi, D. A. (2005). Structural changes in trisilanol POSS during nanocomposite melt processing. *Composite Interfaces*, *11*, 673–685.

Zhang, W., Fu, B. X., Seo, Y., Schrag, E., Hsiao, B., Mather, P. T., Yang, N.-L., Xu, D., Ade, H., Rafailovich, M., & Sokolov, J. (2002). Effect of methyl methacrylate/polyhedral oligomeric silsesquioxane random copolymers in compatibilization of polystyrene and poly(methyl methacrylate) blends. *Macromolecules*, *35*, 8029–8038.

Zhao, J., Fu, Y., & Liu, S. (2008). Polyhedral oligomeric silsesquioxane (POSS)–modified thermoplastic and thermosetting nanocomposites: A review. *Polymers and Polymer Composites*, *16*, 483–500.

Zhao, Y., & Schiraldi, D. A. (2005). Thermal and mechanical properties of polyhedral oligomeric silsesquioxane (POSS)/polycarbonate composites. *Polymer*, *46*, 11640–11647.

Zheng, L., Farris, R. J., & Coughlin, E. B. (2001). Novel polyolefin nanocomposites: Synthesis and characterization of metallocene catalyzed polyolefin polyhedral oligomeric silsesquioxanes (POSS) copolymers. *Macromolecules*, *34*, 8034–8039.

Zhou, Z., Cui, L., Zhang, Y., Zhang, Y., & Yin, N. W. (2008). Preparation and properties of POSS grafted polypropylene by reactive blending. *European Polymer Journal*, *44*, 3057–3066.